Sensors & Transducers, Vol. 22, Special Issue, June 2013, pp. 111-118

www.sensorsportal.com

Sensors & Transducers

http://www.sensorsportal.com

Influence Analysis of Star Sensors' Sampling Frequency on Attitude Determination Accuracy

[1, 2] Yuanyuan Jiao, [1] Xiaogang Pan, [3] Jiongqi Wang, [2] Yong Li, [3] Haiyin Zhou

[1] College NineNational University of Defense Technology, Changsha, China

[2] School of Surveying & Spatial Information Systems, The University of New South Wales, Sydney, Australia

[3] Department of Mathematics and Systems Science, National University of Defense Technology, Changsha, China

E-mails: jyynudt@gmail.com; jyjy0103@163.com

Received: 15 April 2013 /Accepted: 20 June 2013 /Published: 28 June 2013

Abstract: The star sensor has been widely used as an important and accurate attitude measurement sensor in classical satellite attitude determination systems. This paper analyses the influence of star sensor's sampling frequency on attitude determination accuracy within an Extended Kalman filter (EKF). Simulations are used to validate the theoretical analysis and determine the parameters of the influence function. The results show that in most scenarios, the influence of the star sensor's sampling frequency on the attitude determination accuracy can be expressed by the characteristic parameter in the influence function, which is not affected by other accuracy influence factors. *Copyright © 2013 IFSA.*

Keywords: Star sensor, Attitude determination, Sampling frequency, Influence analysis.

1. Introduction

High accuracy attitude determination plays an important role in earth-orientation and satellite control [1]. As input of the attitude determination algorithms, the accuracy of the attitude measurement is regarded as the most important influence factor in determining the satellite's attitude. Since star sensor has the highest measurement accuracy [2, 3], it is the most widely used sensor in satellite attitude determination systems.

Over the past decade, the problem of attitude determination using star sensors has been reported in the research literatures, such as, determining the attitude by a set of observation vectors of star sensors [4-6], and different types of filtering methods using the observation vectors of star sensors together with the measurement of angular velocity [7-9], deep analysis of the star sensor's measurement model, as well as the characteristics of measurement errors [4, 10-12]. In addition to the aspects above, it has been found that the sampling frequency of the star sensor is an important factor that has significant influence on the accuracy of attitude solution. Farrenkopf gave an analytical solution for the steady-state covariance of attitude angle's estimation error for a single-axis Kalman filter [13]. Markley and Reynolds then modified Farrenkopf's results to include the effect of gyro output noise [14], and derived the relationship between the star sensor's sampling interval and the standard deviation of the angular estimation. Based on such work, this paper derives the analytical representation of the influence of the star sensor's sampling frequency on the widely-used EKF-based attitude determination accuracy we defined. The quaternion-based EKF in this paper combines the measurements from three star sensors and gyros.

Since star sensor's measurement accuracy is high, the following attitude determination method is

commonly used. That is, the angular velocity information is used to predict the attitude when the star sensor's measurement data is absent. The attitude is updated when the star sensor's measurement is available. Obviously the star sensor's sampling frequency determines the time span of prediction and updating in the process of attitude determination. Therefore a high sampling frequency can help to increase the attitude determination accuracy. Nevertheless, since the time of exposure and the time of internal circuit and algorithmic processing are restricted, a heavier cost has to be paid for the increase of the star sensor's sampling frequency during design and manufacturing [15]. Therefore, analyzing the influence of star sensor's sampling frequency on the attitude determination accuracy can support the requirement analysis for increasing the star sensor's sampling frequency.

The paper is organized as follows. Following the introduction, the measurement model of attitude sensors and the equations of the EKF-based attitude determination system are presented. The form of the influence function of the star sensor's sampling frequency is then analyzed in Section 3 from a theoretical point of view. In Section 4, simulations are used to validate the theoretical analysis and determine the parameters of the influence function. Furthermore, the parameters in the influence function are estimated and validated in the simulation tests under different conditions. Finally, the paper is concluded in Section 5.

2. Equations of Attitude Determination System

2.1. Measurement Model of Gyros and State Equation of EKF

The gyros' measurement model is first introduced. It is written as [9].

$$\begin{aligned} \omega_g &= \omega_{bi} + b + \eta_g \\ \dot{b} &= \eta_b \end{aligned}, \tag{1}$$

where ω_g is the measured angular velocity. ω_{bi} is the coordinate of the inertial angular velocity of the satellite in the body frame. b denotes the gyro drift. η_g and η_b are independent Gaussian white-noise processes with

$$\begin{aligned} &\mathrm{E}(\eta_k(t)) = 0, \\ &\mathrm{E}(\eta_k(t)\eta_k^{\mathrm{T}}(t')) = \sigma_k^2 \cdot \mathbf{I} \cdot \delta(t-t') \quad (k = g,b), \end{aligned}$$

where $\delta(t-t')$ is the Dirac-delta function.

The EKF state equation can be derived from the quaternion based kinematic equation, and it is constructed by the first three independent components of the error quaternion Δq [16,17], which is defined to represent the rotation from the estimated attitude $\hat{q}$ to the true attitude q. For convenience, the first three independent components are denoted as $\Delta\bar{q}$. With the state vector consisting of $\Delta\bar{q}$ and the estimation error of gyro drift Δb, the state equation for $X_{6\times1} = [\Delta\bar{q}^{\mathrm{T}} \quad \Delta b^{\mathrm{T}}]^{\mathrm{T}}$ is given by [9,16]:

$$\dot{X}(k) = \mathbf{F}(k)X(k) + W(k) \tag{2}$$

where,

$$\mathbf{F}(k) = \begin{bmatrix} -[\hat{\omega}_{bi}\times] & -0.5I_{3\times3} \\ 0_{3\times3} & 0_{3\times3} \end{bmatrix}, [\hat{\omega}\times] = \begin{bmatrix} 0 & -\hat{\omega}_3 & \hat{\omega}_2 \\ \hat{\omega}_3 & 0 & -\hat{\omega}_1 \\ -\hat{\omega}_2 & \hat{\omega}_1 & 0 \end{bmatrix},$$

$$W(k) = \begin{bmatrix} -0.5\eta_g \\ \eta_b \end{bmatrix}.$$

The corresponding discrete form of Equation (2) is

$$\begin{aligned} X(k+1) &= (\mathbf{I} + \Delta t \cdot \mathbf{F}(k))X(k) + \varepsilon(k) \\ &= \mathbf{\Phi}(k+1,k)X(k) + \varepsilon(k) \end{aligned} \tag{3}$$

where ,

$$\varepsilon(k) = \begin{bmatrix} -\frac{1}{2} f_{k+1} & g_{k+1} \end{bmatrix}^{\mathrm{T}} \tag{4}$$

$$f_{k+1} = \int_k^{k+1} (k+1-s)\eta_b(s) + \eta_g(s)ds \tag{5}$$

$$g_{k+1} = \int_k^{k+1} \eta_b(s)ds \tag{6}$$

$$\begin{aligned} &\mathbf{Q} = \mathrm{E}(\varepsilon(k)\varepsilon(k)^{\mathrm{T}}) \\ &= \begin{bmatrix} (\frac{1}{12}\sigma_b^2 \cdot \Delta t^3 + \frac{\Delta t}{4} \cdot \sigma_g^2) \cdot \mathbf{I}_{3\times3} & \frac{1}{4}\sigma_b^2 \cdot \Delta t^2 \cdot \mathbf{I}_{3\times3} \\ \frac{1}{4}\sigma_b^2 \cdot \Delta t^2 \cdot \mathbf{I}_{3\times3} & \Delta t \cdot \sigma_b^2 \cdot \mathbf{I}_{3\times3} \end{bmatrix} \end{aligned} \tag{7}$$

2.2. Measurement Model of Star Sensors and Measurement Equation of EKF

Assumed that three star sensors are mounted on the three axes of the body frame of a satellite, the measurement equation of the star sensors' optical axes is given as [11, 16, 17]:

$$\boldsymbol{Z}(k) = \boldsymbol{h}(q,l) + \boldsymbol{V}(k), \tag{8}$$

where

$$\boldsymbol{h}(\boldsymbol{q},\boldsymbol{l})=\begin{bmatrix}\boldsymbol{l}_{iz1}\\ \boldsymbol{l}_{iz2}\\ \boldsymbol{l}_{iz3}\end{bmatrix}=\begin{bmatrix}\boldsymbol{h}_1=\boldsymbol{A}_{bi}{}^{\mathrm{T}}(\boldsymbol{q})\boldsymbol{l}_{bz1}\\ \boldsymbol{h}_2=\boldsymbol{A}_{bi}{}^{\mathrm{T}}(\boldsymbol{q})\boldsymbol{l}_{bz2}\\ \boldsymbol{h}_3=\boldsymbol{A}_{bi}{}^{\mathrm{T}}(\boldsymbol{q})l_{bz3}\end{bmatrix}.$$

In the above equations, $\boldsymbol{A}_{bi}{}^{\mathrm{T}}(q)$ is the transfer matrix from the body frame to the inertial frame, and q is the corresponding attitude quaternion. $\boldsymbol{l}_{bzj},\boldsymbol{l}_{izj}$, ($j=1,2,3$) are the coordinates of the star sensors' optical axes in the body frame and inertial frame respectively. $\boldsymbol{V}(k)$ is the measurement random noise sequence, its covariance matrix is $\mathbf{R}$.

Based on the star sensors' measurement model, the measurement equation for $X_{6\times1}=[\Delta\overline{q}^{\mathrm{T}}\ \ \Delta b^{\mathrm{T}}]^{\mathrm{T}}$ is written as [16, 17]

$$\boldsymbol{Y}_k=\widehat{\mathbf{H}}_k\boldsymbol{X}(k)+\boldsymbol{V}_k \tag{9}$$

where

$$\boldsymbol{Y}_k=\left[\boldsymbol{Z}_k(1)-\mathbf{A}_{bi}^{\mathrm{T}}(\hat{q})\boldsymbol{l}_{bz1}\quad \boldsymbol{Z}_k(2)-\mathbf{A}_{bi}^{\mathrm{T}}(\hat{q})\boldsymbol{l}_{bz2}\quad \boldsymbol{Z}_k(3)-\mathbf{A}_{bi}^{\mathrm{T}}(\hat{q})\boldsymbol{l}_{bz3}\right]^{\mathrm{T}},$$

$\boldsymbol{Z}_k(j)$ is the j^{th} element of $Z(k)$,

$$\widehat{\mathbf{H}}_k=\begin{bmatrix}\mathbf{H_1} & \mathbf{0}\\ \mathbf{H_2} & \mathbf{0}\\ \mathbf{H_3} & \mathbf{0}\end{bmatrix}=\begin{bmatrix}-2\mathbf{A}_{bi}^{\mathrm{T}}(\hat{q})[l_{bz1}\times] & 0\\ -2\mathbf{A}_{bi}^{\mathrm{T}}(\hat{q})[l_{bz2}\times] & 0\\ -2\mathbf{A}_{bi}^{\mathrm{T}}(\hat{q})[l_{bz3}\times] & 0\end{bmatrix}.$$

3. Analysis of the Influence of Star Sensor's Sampling Frequency

According to the formula of the EKF-based attitude determination algorithm [16], together with Equation. (9) and Equation. (2)-(7), one can see that the influence of the star sensor's sampling frequency on the EKF-based attitude determination method is mainly represented by the state transformation matrix $\boldsymbol{\Phi}(k,k-1)$ and covariance matrix of process noise $\mathbf{Q}$.

Before analyzing the influence of star sensor's sampling frequency, a criterion is defined to measure the accuracy of attitude determination. $\mathbf{P}(k/k)$ is the covariance matrix of estimate error. Since only the accuracy of the satellite attitude is of concern, the trace of the first three dimensions of the covariance matrix $\mathbf{P}(k/k)$ can be used as the measure of attitude estimation accuracy. For convenience, the sub-matrix constructed by the first three dimensions of matrix $\mathbf{P}$ is denoted as $\ddot{\mathbf{P}}$. The trace of $\ddot{\mathbf{P}}$ is denoted as $\mathrm{t\ddot{r}}(\mathbf{P})$, which is the criterion of measuring the accuracy of attitude determination.

According to the formulation of the EKF

$$\begin{aligned}&\mathbf{P}(k/k)=\mathbf{P}(k/k-1)-\mathbf{K}(k)\widehat{\mathbf{H}}(k)\mathbf{P}(k/k-1)\\ &=\boldsymbol{\Phi}(k/k-1)\mathbf{P}(k-1/k-1)\boldsymbol{\Phi}^{\mathrm{T}}(k/k-1)+\mathbf{Q}(k-1)\\ &-\mathbf{P}(k/k)\widehat{\mathbf{H}}^{\mathrm{T}}(k)\mathbf{R}_k^{-1}\widehat{\mathbf{H}}(k)(\boldsymbol{\Phi}(k/k-1)\mathbf{P}(k-1/k-1)\boldsymbol{\Phi}^{\mathrm{T}}(k/k-1)+\mathbf{Q}(k-1))\end{aligned} \tag{10}$$

Denote

$$\boldsymbol{\Psi}_{k/k-1}=\boldsymbol{\Phi}(k/k-1)\boldsymbol{\Phi}^{\mathrm{T}}(k/k-1),$$
$$\boldsymbol{\Theta}_k=\widehat{\mathbf{H}}^{\mathrm{T}}(k)\widehat{\mathbf{H}}(k),\ \mathbf{R}_k=r\cdot\mathbf{I}\ .$$

The accuracy metric $\mathrm{t\ddot{r}}(\mathbf{P}(k/k))$ can be written as

$$\begin{aligned}&\mathrm{t\ddot{r}}(\mathbf{P}(k/k))=\mathrm{t\ddot{r}}(\boldsymbol{\Psi}_{k/k-1}\mathbf{P}(k-1/k-1))+\mathrm{t\ddot{r}}(\mathbf{Q}_{k-1})\\ &-\mathrm{t\ddot{r}}(\mathbf{P}(k/k)\boldsymbol{\Theta}_k\mathbf{R}_k^{-1}\boldsymbol{\Psi}_{k/k-1}\mathbf{P}(k-1/k-1))-\mathrm{t\ddot{r}}(\mathbf{P}(k/k)\boldsymbol{\Theta}_k\mathbf{R}_k^{-1}\mathbf{Q}_{k-1})\end{aligned} \tag{11}$$

Combining with Equation (3), one can obtain

$$\ddot{\boldsymbol{\Psi}}_{k/k-1}=\begin{bmatrix}1+\Delta t^2\hat{\omega}_3^2+\Delta t^2\hat{\omega}_2^2+0.25\Delta t^2 & -\Delta t^2\hat{\omega}_1\hat{\omega}_2 & -\Delta t^2\hat{\omega}_1\hat{\omega}_3\\ -\Delta t^2\hat{\omega}_1\hat{\omega}_2 & 1+\Delta t^2\hat{\omega}_1^2+\Delta t^2\hat{\omega}_3^2+0.25\Delta t^2 & -\Delta t^2\hat{\omega}_2\hat{\omega}_3\\ -\Delta t^2\hat{\omega}_1\hat{\omega}_3 & -\Delta t^2\hat{\omega}_2\hat{\omega}_3 & 1+\Delta t^2\hat{\omega}_1^2+\Delta t^2\hat{\omega}_2^2+0.25\Delta t^2\end{bmatrix} \tag{12}$$

Considering that the rotating angular velocity of the satellite is usually small, $\ddot{\boldsymbol{\Psi}}_{k/k-1}=(\Psi)_{ii}$ can be approximated by a diagonal matrix.

Denote the element in the ith row and the jth column of attitude matrix $\mathbf{A}$ as $a_{ij},i,j=1,2,3$. Since the directions of the star sensors' optical axes are aligned with the axes of the body frame, one can obtain the observation matrix by combining them with the form of the observation matrix

$$\mathbf{H}_1=-2\begin{bmatrix}0 & a_{31} & -a_{21}\\ 0 & a_{32} & -a_{22}\\ 0 & a_{33} & -a_{23}\end{bmatrix},$$
$$\mathbf{H}_2=-2\begin{bmatrix}-a_{31} & 0 & a_{11}\\ -a_{32} & 0 & a_{12}\\ -a_{33} & 0 & a_{13}\end{bmatrix},$$
$$\mathbf{H}_3=-2\begin{bmatrix}a_{21} & -a_{11} & 0\\ a_{22} & -a_{12} & 0\\ a_{23} & -a_{13} & 0\end{bmatrix}.$$

Thus,

$$\boldsymbol{\Theta}_k=\widehat{\mathbf{H}}_k^{\mathrm{T}}\widehat{\mathbf{H}}_k=\begin{bmatrix}8 & 0 & 0 & 0_{1\times3}\\ 0 & 8 & 0 & 0_{1\times3}\\ 0 & 0 & 8 & 0_{1\times3}\\ 0_{3\times1} & 0_{3\times1} & 0_{3\times1} & 0_{3\times3}\end{bmatrix} \tag{13}$$

Then,

$$\ddot{\mathrm{t}}(\mathbf{P}(k/k)) = \sum_{i=1}^{3} p(k)_{ii} = \sum_{i=1}^{3} p(k-1)_{ii}\Psi_{ii} + \sum_{i=1}^{3} Q_{ii} - \frac{1}{r}\cdot 8\cdot \sum_{i=1}^{3}(p(k)_{ii}\cdot p(k-1)_{ii}\Psi_{ii}) - \frac{1}{r}\cdot 8\cdot \sum_{i=1}^{3} p(k)_{ii} Q_{ii} \tag{14}$$

Considering that the Kalman filter will converge to the steady-state, one can assume that the covariance after processing all these measurements, $\mathbf{P}(k/k)$, is identical with the covariance $\mathbf{P}(k-1/k-1)$ [14]. Furthermore, using the average value of the first three diagonal components of matrix **P** as the accuracy index y, Equation (14) can be rewritten as

$$3y = y\cdot\sum_{i=1}^{3}\Psi_{ii} + \sum_{i=1}^{3} Q_{ii} - \frac{8}{r}y^2\sum_{i=1}^{3}\Psi_{ii} - \frac{8}{r}y\sum_{i=1}^{3} Q_{ii} \tag{15}$$

Substituting Equation (3-7) and Equation (12), one obtains

$$\frac{8}{r}(3+(2(\hat{\omega}_1^2+\hat{\omega}_2^2+\hat{\omega}_3^2)+0.75)\cdot\Delta t^2)\cdot y^2 + (\frac{2}{r}\sigma_b^2\cdot\Delta t^3 + \frac{6}{r}\cdot\sigma_g^2\cdot\Delta t - (2(\hat{\omega}_1^2+\hat{\omega}_2^2+\hat{\omega}_3^2)+0.75)\cdot\Delta t^2)\cdot y - (\frac{1}{4}\sigma_b^2\cdot\Delta t^3 + \frac{3}{4}\cdot\sigma_g^2\cdot\Delta t) = 0 \tag{16}$$

The solution of this quadratic equation represents the relationship between the accuracy index y and the star sensor's sampling interval Δt. It is a polynomial with respect to Δt. Nevertheless, its concrete form is too complex to use. Since the order of Δt in this solution is between -2 and 1, we use the equation $y = p_1\Delta t^{p_2} + p_3, -2 \le p_2 \le 1$ as the form of approximated solution, i.e., the influence function model, where p_3 is 0. It can be derived from Equation (16) as Δt approaches to 0. Since the star sensor's sampling frequency is $x = 1/\Delta t$, the influence function model of the star sensor's sampling frequency and the square root of y (used as the final accuracy index) is as follows: $y = p_1 x^{p_2}, -1/2 \le p_2 \le 1$.

Notice that when the star sensors' mounting direction is changed, if they are still orthogonal, according to the form of observation matrix, the analysis result is the same as described above. But if they are not orthogonal, then the diagonal element is unchanged, but the off-diagonal elements of $\mathbf{\Theta}_k$ are the cosine values of the angles between every pair of optical axes. Commonly, the angle is still nearly 90 degree, hence compared to the diagonal elements, the off-diagonal elements of $\mathbf{\Theta}_k$ are very small. Then, $\ddot{\mathbf{\Theta}}_k$ can still be assumed to be a diagonal matrix. This will not affect the above result significantly.

4. Simulated Experiments

Four sets of experiments with different conditions are used to validate the theoretical analysis.

It is known that the estimated errors of the quaternion and attitude angles have a linear relationship when the estimated error is small. Meanwhile, the estimated accuracy of the attitude angles is commonly employed to measure the performance. Therefore, instead of the accuracy index represented by error quaternion, the average of the attitude angles' estimated error is used as the metric in the simulations. This replacement will not change the form of the influence function.

4.1. Experiment 1

(1) The standard deviation of the gyros' measurement noise and constant drift noise is $\sigma_g = 0.05\,\mathrm{deg/h}$ and $\sigma_b = 0.03\,\mathrm{deg/h}$. The gyro constant drift is assumed to be $b = [1,-1,1]^{\mathrm{T}}$ deg/h.

(2) The measurement accuracy of the star sensor is assumed to be $10''(3\sigma)$. The mounting direction of the star sensors' axes align with the body frame's three axes.

Under the above assumed conditions, the experiment is conducted by choosing 11 experimental points in which the star sensor's sampling frequency is varied from 0.2 Hz to 20 Hz.

According to the experimental results, the influence of the star sensor's sampling frequency on EKF-based attitude determination accuracy is shown in Fig. 1.

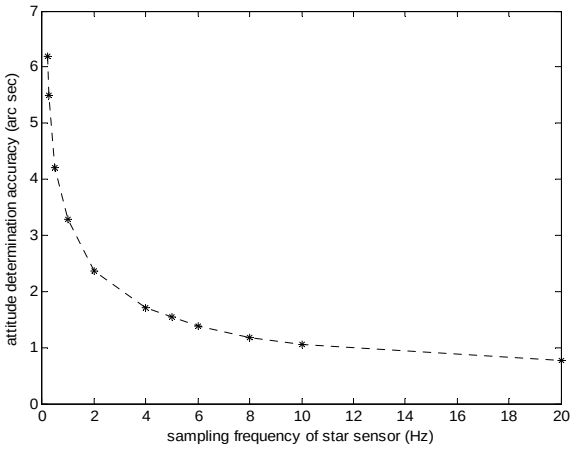

Fig. 1. EKF based attitude determination accuracy with different star sensor's sampling frequency. (Star sensor's measurement accuracy is 10 arc sec.).

As can be seen from Fig. 1, the curve has a negative exponential form. This characterizes the influence of the star sensor's sampling frequency on attitude determination accuracy, which is also

consistent with the results of theoretical analysis, i.e. this undetermined influence function can be modeled as the negative exponential function

$$y = p_1 x^{p_2}, -1 \le p_2 < 0 \quad (17)$$

The task is now to estimate the parameters, i.e. p_1 and p_2. From Equation (17), the model can be transformed into the form $\ln y = \ln p_1 - p_2 \ln x$. Then, the parameter p_2 can be estimated as p_2 =-0.451 in this experiment by using the principle of least squares fitting. Therefore, the inverse proportional function model $y = p_1 / x^{0.45}$ can be used as star sensor's sampling frequency influence function. Similarly, the parameter p_1 can be estimated as p_1 =3.038 using the experimental results. Thus the influence function between the star sensor's sampling frequency *x* and the EKF-based attitude determination accuracy y under the experimental condition has been established, i.e. $y = 3.038 / x^{0.45}$.

In order to verify the validity of this influence function, the curve of the influence function derived above is plotted in Fig. 2. In addition, the curve based on the experimental results (shown in Fig. 1) is also plotted in Fig. 2 for easy comparison. Correspondingly, the fitting errors for all experimental points are listed in the first row of Table 1.

Table 1. The influence function's fitting errors with different measurement accuracy (arc sec).

Exp.	1	2	3	4	5	6	7	8	9	10	11
Star sensor 10 arc sec	0.080	0.173	0.048	0.255	0.140	0.077	0.067	0.032	0.017	0.034	0.020
Star sensor 18 arc sec	0.162	0.280	0.074	0.278	0.089	0.019	0.056	0.050	0.085	0.118	0.00006
Star sensor 30 arc sec	0.520	0.451	0.340	0.514	0.039	0.053	0.008	0.146	0.210	0.261	0.155

From Fig. 2, it is evident that the curves of the influence function and experimental results almost overlap. Moreover, data in the first row of Table 1 also shows that the fitting error at every experimental point limits. This means that the derived influence function model can effectively reflect the relationship between the star sensor's sampling frequency and the EKF-based attitude determination accuracy under this experimental condition.

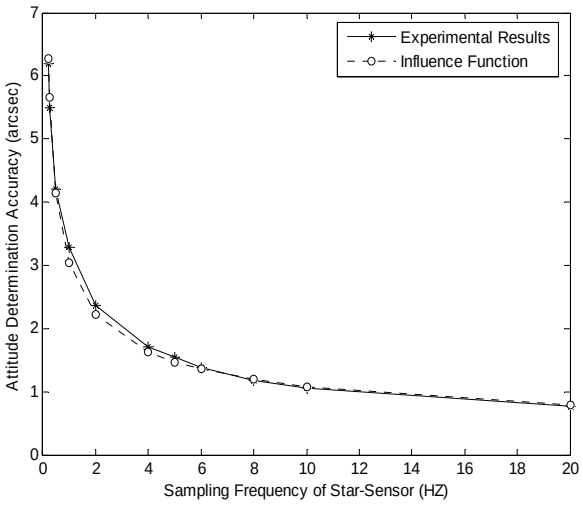

Fig. 2. Comparison between the influence function and experiment results. (Star sensor's measurement accuracy is 10 arc sec.).

4.2. Experiment 2

This experiment mainly investigates the influence function in relation to different star sensor's measurement accuracy.

With the same experimental conditions as in Experiment 1, experiments are conducted with the measurement accuracies of $18''(3\sigma)$ and $30''(3\sigma)$. The same method as in Experiment 1 is used to determine the parameters of the influence function. When the measurement accuracy is $18''(3\sigma)$, the influence function is $y = 4.897 / x^{0.45}$. When the measurement accuracy is $30''(3\sigma)$, it becomes $y = 7.374 / x^{0.45}$. Similarly, for different measurement errors, the fitting errors between influence functions and the experimental results at different experimental points are listed in rows 2 and 3 of Table 1.

As seen from the Table 1, when the measurement accuracy is $18''(3\sigma)$, the fitting errors at every experimental point are mostly smaller than $0.3''(3\sigma)$. When the measurement error is $30''(3\sigma)$, the fitting errors are all bounded by $0.5''(3\sigma)$. This reflects the fact that our derived influence functions are consistent with the experimental results, even with different measurement errors. It also verifies the fact that the form of the influence function we analyzed can

effectively represent the influence of star sensor's sampling frequency on the EKF-based attitude determination accuracy.

Fig. 3 illustrates that the curves of the influence functions relating the star sensor's sampling frequency and attitude determination accuracy with different measurement accuracies, i.e., 10 arc sec (3σ), 18 arc sec (3σ) and 30 arc sec (3σ).

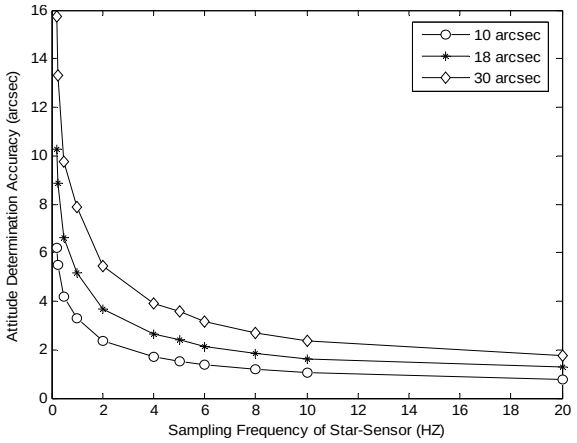

Fig. 3. EKF based attitude determination accuracy with different star sensor's sampling frequency and measurement accuracies.

Based on the results in Fig. 3, the forms of the influence functions are the same as Equation (17). More interestingly, after repeating every experiment several times, it is found that the degree of the variable *x* in the influence function is usually -0.45, which is consistent with the theoretical analysis. According to the properties of the exponential function family, this parameter determines the function's shape. In other words it is the intrinsic characteristic of the influence relating the star sensor's sampling frequency and the attitude determination accuracy. It doesn't change with respect to star sensor's measurement accuracy. Thus it can be considered the "characteristic parameter". The other parameter is changed for different simulation conditions. It may depend on other factors, such as the measurement accuracy. It is referred to as the "scale parameter." As seen from Fig. 3, the scale parameter increases with decrease of measurement accuracy.

From Experiment 2 the conclusion can be drawn that the characteristic parameter of the influence function is -0.45 and it determines the influence trend of the star sensor's sampling frequency on the EKF-based attitude determination accuracy. The scale parameter, however, is closely related to other factors such as the measurement accuracy.

4.3. Experiment 3

This experiment is to validate whether the influence law changes with different values of other factors such as gyros' measurement accuracy and star sensor's mounting direction.

First, the influence of gyros' measurement accuracy is investigated. All kinds of gyros' noise are changed to $0.03^\circ/h$, and other conditions remained the same as in Experiment 1. Then, the mounting direction of the star sensors is changed as:

$$\theta = 30^\circ, l_{bz1} = \left[\cos\theta \quad 0 \quad \sin\theta\right]^{\mathrm{T}},$$

$$l_{bzk} = \left[-\sin 30^\circ \cos\theta \quad (-1)^k \cos 30^\circ \cos\theta \quad \sin\theta\right]^{\mathrm{T}}, k = 2,3$$

With changing the gyros' measurement accuracy and the mounting direction of star sensor, Fig. 4 depicts curves of influence function between star sensor's sampling frequency and attitude determination accuracy.

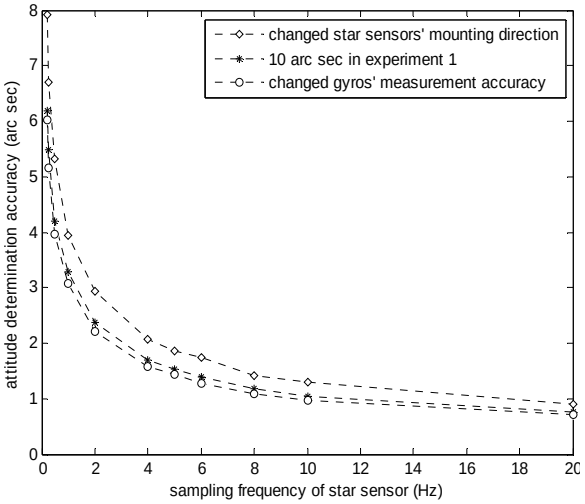

Fig. 4. The influence relations between star sensor's sampling frequency and attitude determination accuracy with gyro's measurement accuracy and star sensors' mounting direction changed.

Fig. 4 shows that when the gyro's measurement accuracy and the star sensor's mounting direction are changed, the form of the influence function relating star sensor's sampling frequency and attitude determination accuracy is still $y = p_1 x^{p_2}$. A similar method as in Experiment 1 is used to estimate the parameters in the influence functions, they are $y = 2.885 / x^{0.45}$ and $y = 3.786 / x^{0.45}$ respectively. Furthermore, the fitting errors between the influence function and the experimental data at each experimental point are calculated, and the results are listed in Table 2.

As seen from Table 2, when the gyro's measurement accuracy and the mounting direction of the star sensor are changed, the maximum fitting error between the influence functions of the star sensor's sampling frequency and the experimental results is about $0.3''(3\sigma)$.

Table 2. The influence function's fitting errors with different simulation conditions (arc sec).

Exp.	1	2	3	4	5	6	7	8	9	10	11
Changed gyros' accuracy	0.078	0.235	0.016	0.180	0.106	0.042	0.047	0.010	0.037	0.058	0.0323
Changed star sensors' mounting direction	0.105	0.373	0.156	0.149	0.155	0.032	0.027	0.047	0.070	0.043	0.078

Together with the previous two experiments, the results indicate that simulated experiments with different conditions show the validation of influence function model and its estimated parameters. Concretely, the results show that: (1) the influence function model constructed can effectively reflect the influence of the star sensor's sampling frequency on attitude determination accuracy for different situations. (2) The influence of the star sensor's sampling frequency on the attitude determination accuracy is mostly represented by the characteristic parameter p_2 =-0.45. In most scenarios, this parameter does not change with other influence factors.

4.4. Experiment 4

The first three groups of experiments are focus on theoretical analysis validation. Thus, the simulated attitude data is created by attitude kinematic equation with an initial quaternion parameter and a set of angular velocity information. In this group of experiment, attitude data of on orbit satellite is derived from STK software. Then, this on orbit data is used to verify the previous conclusions deeply. The concrete parameters in STK are listed as follows: for a GEO satellite, the semi major axis is 42164.1696 km, eccentricity is 0 degree, inclination is 0 degree, argument of perigee is 0 degree, longitude of ascending node is 260 degree, true anomaly is 0 degree. The propagator used is J2 perturbation. Reference attitude is used nadir alignment with ECI velocity. The initial quaternion is 0.181783, 0.683341, 0.181246, 0.683484. The initial angular velocity is 0.000008376 deg/sec, -0.0000047866 deg/sec, -0.0209259 deg/sec.

The attitude data is derived with 0.5 Hz, 1 Hz, 2 Hz, 4 Hz, 8 Hz and 10 Hz. The attitude estimation results are plotted by real line in Fig. 5. The model $y = p_1 x^{p_2}$, p_2=0.45 is still used as the influence function, then p_1=3.7939 can be obtained as in previous experiments.

For comparison, the results computed by the influence function directly are also drawn in Fig. 5. The corresponding fitting error is listed in Table 3. They are basically within 10% of attitude estimated error.

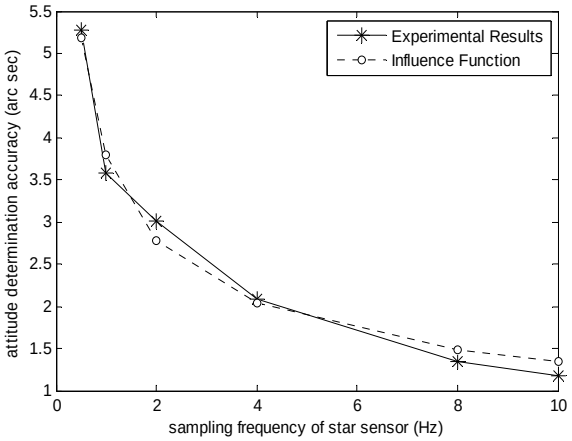

Fig. 5. Comparison between the influence function and experiment results (STK).

These results show that the form of influence function, which describes the relationship between star sensors's sampling frequency and attitude determination accuracy, is reasonable. And the characteristic parameter in the influence function, p_2 =-0.45, is valid even with the on orbit simulated data.

Table 3. The influence function's fitting errors with STK (arc sec).

Exp.	1	2	3	4	5	6
STK	0.089	0.209	0.232	0.060	0.148	0.161

5. Conclusions

This paper analyzed the influence of the star sensor's sampling frequency on the EKF-based attitude determination accuracy. Theoretical analysis was used to construct the form of the influence function, and the simulation experiments were employed to determine the parameters of this

function. The influence functions relating the star sensor's sampling frequency and attitude determination accuracy under different conditions were determined. The influence function was verified by the precise fitting between the influence function and the experimental data in simulation experiments under different conditions. The results show that the influence on attitude determination accuracy of the star sensor's sampling frequency is mostly represented by the characteristic parameter in the influence function, i.e. p_2 =-0.45. The scale parameter p_1 in the influence function changes with other influence factors, while the characteristic parameter p_2 is a constant.

Acknowledgements

This work is supported by NSFC China (No. 61004081, 60904098 and 11126033). The authors would like to thank reviewers and Professor Chris Rizos in University of New South Wales for their constructive suggestions.

References

[1]. M. E. Pittelkau, Kalman Filtering for Spacecraft System Alignment Calibration, *Journal of Guidance, Control, and Dynamics*, Vol. 24, No. 6, 2001, pp. 1187–1195.

[2]. S. Tu, Satellite Attitude Dynamic and Control, *Chinese Astronautics Press*, Beijing, 2005.

[3]. L. Blarre, J. Ouaknine, L. Oddos-Marcel, et al., High accuracy Sodern Star Trackers: Recent improvements proposed on SED36 and HYDRA star Trackers, in *Proceedings of the AIAA Guidance, Navigation, and Control Conference*, Keystone, CO, United States, 6046, 2006, pp. 132-138.

[4]. M. D. Shuster, S. D. Oh, Three-Axis Attitude Determination from Vector Observations, *Journal of Guidance, Control, and Dynamics*, Vol. 4, No. 1, 1981, pp. 70-77.

[5]. I. Y. Bar-Itzhack and Y. Oshman, Attitude Determination from Vector Observations: Quaternion Estimation, *IEEE Transactions on Aerospace and Electronic Systems*, Vol. AES-21, No. 1, 1985, pp. 128–136.

[6]. Y. Cheng, J. L. Crassidis, and F. L. Markley, Attitude Estimation for Large Field-of-View Sensors, *AAS Paper*, 2005, 05-462.

[7]. M. L. Psiaki, Attitude-Determination Filtering via Extended Quternion Estimation, *Journal of Guidance, Control, and Dynamics*, Vol. 23, No. 2, 2000, pp. 206-214.

[8]. I. Kim, J. Kim, and Y. Kim, Angular Rate Estimator Using Disturbance Accommodation Technique, *AIAA Paper*, 2002, 4829.

[9]. J. L. Crassidis, F. L. Markley, and Y. Cheng, Survey of Nonlinear Attitude Estimation Methods, *Journal of Guidance, Control, and Dynamics*, Vol. 30, No. 1, 2007, pp. 12-28.

[10]. M. D. Shuster, Kalman Filtering of Spacecraft Attitude and the QUEST Model, *Journal of the Astronautical Sciences*, Vol. 38, No. 3, 1990, pp. 377-393.

[11]. Y. Liu, Y. Chen, Star-sensor measurement model and its application to the spacecraft attitude determination system, *Journal of Astronautics*, Vol. 24, No. 2, 2003, pp. 162-167.

[12]. Y. Jiao, H. Zhou, X. Li, J. Wang, X. Pan, Cone Measurement Error Model of Star-sensor's Optic Axis and Its Application, *Journal of Astronautics*, Vol. 31, No. 9, 2010, pp. 2138-2144.

[13]. R. L. Farrenkopf, Analytic Steady-State Accuracy Solutions for Two Common Spacecraft Attitude Estimators, *Journal of Guidance and Control*, Vol. 1, No 4, 1978, pp. 282-284.

[14]. F. L. Markley and R. G. Reynolds, Analytic Steady-State Accuracy of a Spacecraft Attitude Estimator, *Journal of Guidance, Control, and Dynamics*, Vol. 23, No. 6, 2000, pp. 1065–1067.

[15]. G. Ju and J. L. Junkins, Overview of Star Tracker Technology and its Trends in Research and Development, in *Proceedings of the Advances in the Astronautical Sciences, The John L. Junkins Astrodynamics Symposium*, Vol. 115, AAS-03-285, 2003, pp. 461-478.

[16]. L. Li, Research on the Satellite Autonomous Navigation and Attitude Determination Technology, Postdoctoral Dissertation of Space Science and Application Research Center, *Chinese Academy of Science*, 2003.

[17]. E. J. Lefferts, F. L. Markley, and M. D. Shuster, Kalman Filtering for Spacecraft Attitude Estimation, *Journal of Guidance, Control, and Dynamics*, Vol. 5, No. 5, 1982, pp. 417–429.